3D Elastostatic Thermal-Structural Analysis of the Tubesheet in a U-tube Heat-exchanger and Consequent Flexibility Analysis of Typical U-tubes

Y. S. GARUD, K. E. WATKINS
S. Levy Incorporated, Campbell, CA USA

1 INTRODUCTION AND OBJECTIVES

The recirculating U–tube type design of a steam generator in a pressurized water reactor (PWR) system typically consists of thousands of tubes expansion-fitted in a thick circular plate (tubesheet). The integrity of these pressure retaining tubes, under operating temperatures (around 588° K) and high purity water environments, has been affected by the stress corrosion cracking (SCC), especially, within the transition zone (near the *tube-to-tubesheet* junction). The local stress is a key factor to be considered in resolving or assessing the SCC. For instance, the peaks and gradients of axial and hoop stresses in the SCC-prone zone are expected to influence the location, time to initiation, orientation, and growth-rate of the SCC—with subsequent implications for crack-arrest and/or leak-before-break response. Also, the stress description is essential to relate or interpret the SCC field experience vis-à-vis the (accelerated) laboratory test data.

There are two main sources of the stress: one, the fabrication procedure resulting in the pre-service (residual) stress and two, the operating thermal and pressure loads applied during the service. Work presented in this paper addresses only the operating loads and their effect on stresses and deformations. For the purpose of analysis of the complex assembly of tubes bundled with the steam generator shells a *sub-structuring* approach has been adopted in which the local stresses (within the transition zone) are further separated and analyzed in two parts: (1) stress resulting from the *global* structural reaction of the tubesheet, its attachments, and the tube-bundle and (2) stress in a typical cell of *single* tube-end assembly within a short collar piece cut-out from the tubesheet and subject to the thermal and pressure loads *across the tube wall*. This paper deals with the first part while the second part is presented in the companion paper (Garud, 1991).

The primary objective of this paper is to identify major global factors and their contributions to the significant stresses near the tube-to-tubesheet junction. Other related objectives of interest are (a) to determine the displacement response of the tubesheet (with its attachments including the divider plate) under the normal operating conditions of pressure and temperatures and (b) to calculate the resulting tube loads and the displacement profiles for typical full-length U-tubes.

The following analysis was performed on a typical model-D (Westinghouse) type recirculating U-tube steam generator. Details of analysis and the results are presented in two main sections: (1) the analysis of tubesheet and attached shells without tubes and (2) the analysis of typical full-length tubes with related end conditions and support plate constraining conditions. The thermal analysis assumes steady state conditions and the structural analysis assumes linear elasticity.

2 3D THERMAL-STRUCTURAL ANALYSIS OF TUBESHEET & ATTACHMENTS

2.1 Geometry and model description

The tubesheet and its attachments are modeled as an integral assembly of four parts as illustrated in Fig. 1. All four parts of the geometry were discretized by using the three-dimensional eight-

noded isoparametric solid-brick elements (element type STIF14 of the LIBRA Code [S. Levy Incorporated, 1989]). Note that only half the structure needs to be modeled due to the load–geometric symmetry. The material specifications are: (a) channel head - steel casting [SA 216 Gr.WCC], (b) divider plate - Ni-Cr-Fe Alloy 600 [SB 168], (c) tubesheet - steel forging [SA 508 Cl.2], and (d) stub barrel - carbon steel [SA 533 Gr.A Cl.2].

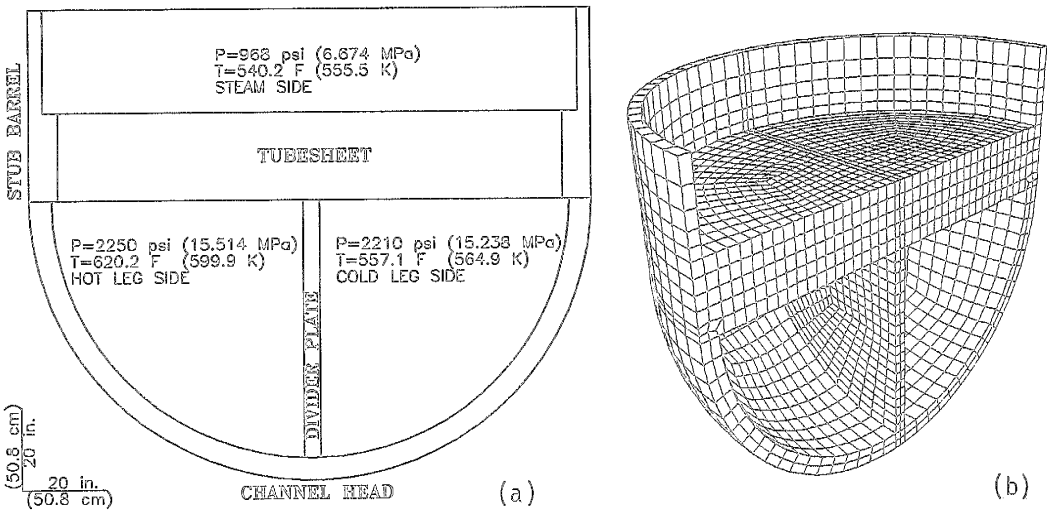

Fig. 1. (a) 4-parts scaled geometry (viewed along the divider plate) and (b) the 3D finite element model perspective of the tubesheet and attachments.

The subsequent analysis and the finite element idealization of the real steam generator are based on the following assumptions: (a) Effects of man-holes and nozzles on the overall displacements and the corresponding loads imposed by the structure were neglected. (b) The top portion of the steam generator was replaced by an effective *constraint* on the top cross-section of the stub barrel such that the (horizontal) section was allowed to move uniformly along the (vertical) axis. (c) The tube bundle offered very little support (or resistance) to the overall structural deformations. This was confirmed by an approximate hand calculation, following Gardner (1960), which yielded a small value for the measure of barreling rigidity of the tube bundle relative to the flexural rigidity of the tubesheet. (d) The perforated tubesheet was replaced by an "equivalent" solid plate with appropriately modified elastic constants. In this case, for the square pitch of 27 mm (1.0625 in.) for the tube holes, the needed constants were estimated to be 39 percent of the original modulus of elasticity and the Poisson's ratio of 0.33. This estimation assumed a partial contribution to the plate rigidity from the embedded tube-ends within the tubesheet. (e) The material properties for each of the parts were assumed to be the Code specified values (ASME, 1980); their temperature dependence was explicitly incorporated in the analysis. (f) For a typical Model–D steam generator the normal pressure and thermal conditions were as defined in Fig. 1(a).

2.2 Results and discussion

The three-dimensional finite element model was analyzed using the pc-based LIBRA computer code; the analysis was performed in two parts: (1) steady state thermal (i.e., heat transfer) solution was obtained generating the nodal temperatures and (2) elasto-static structural solution was obtained by imposing the nodal temperatures and the pressure loads (Fig. 1).

The resultant out-of-plane displacements of the top surface of tubesheet are shown in Fig. 2 as a contour map. The displacement was calculated relative to the center point of the full tubesheet top. This plot indicates a measurable hump (or a deflection peak) located in the cold leg side on the plane of symmetry.

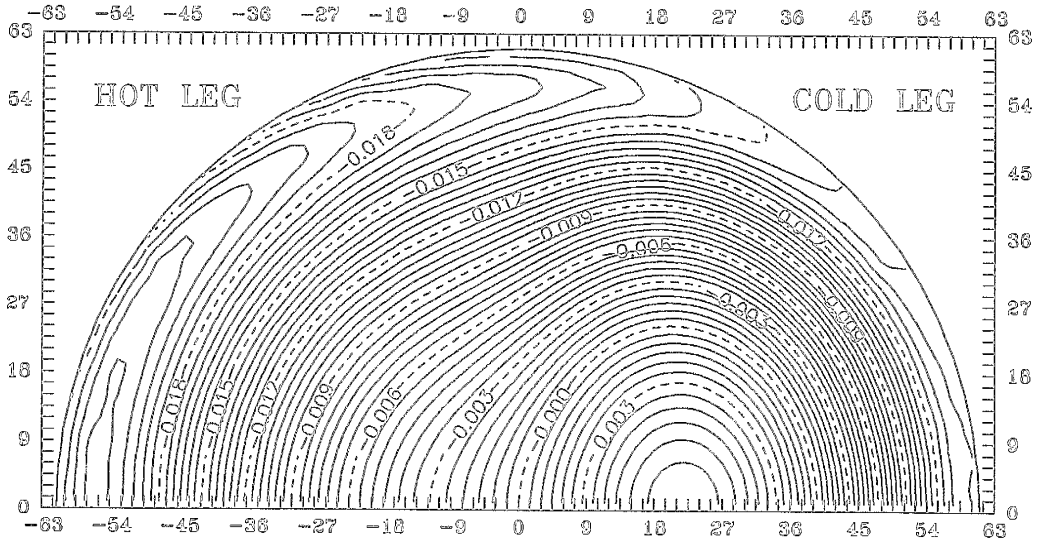

Fig. 2. Vertical relative displacement of the top surface of tubesheet (all dimensions in inches: 1 in. = 25.4mm); the positive displacement is towards the secondary side.

The above response surface can be rationalized as follows: In the absence of divider plate the deflected surface is expected to be nearly spherical (with zero slope at the center). With the divider plate, however, the cold-leg-to-hot-leg thermal difference induces a *lateral* push from hot leg to the cold side of the tubesheet. This push, in effect, over-compensates the normal (concave downward) thermal deflection (due to the gradient from primary to secondary faces) and helps the deflection due to pressure differential; the effect is most pronounced near the divider plate region of the cold leg.

The maximum upward (positive) displacement was found to be about 0.152 mm near the cold leg center and the maximum downward (negative) displacement of about 0.525 mm near the shell-edge of the hot leg. Also, the maximum slope (i.e., the flexural rotation) of the deformed top surface in the direction of a tube lane (parallel to the divider plate plane) was estimated to be about 0.0006 radians; similarly, the maximum slope across the tube lanes (perpendicular to the divider plate plane) was about 0.0008 radians. Although these maxima occur at different locations on the tubesheet surface, for purposes of the subsequent analysis only one resultant maximum flexural rotation was conservatively calculated by assuming the maxima to coincide; i.e., the upper bound value for the rotation was estimated at 0.001 radians (0.058 deg.).

The in-plane (radially outward) displacement of the tubesheet top was found to vary linearly with the radial distance; this is expected because of the nearly uniform (constant) temperature of the top surface. The maximum radial displacement was about 5.842 mm at the periphery of the tubesheet. The average radial expansion of the tubesheet, as computed by the finite element model including shell attachments, is very close to that computed by considering the *free* expansion of tubesheet alone; therefore, it may be concluded that the shell structure as a whole offers negligible thermal restraint on the (axisymmetric) radial expansion of the tubesheet.

These results provide the end conditions for typical tubes analyzed in the following section; for convenience, Table 1 summarizes the displacements and rotations imposed on three tube locations.

Table 1. Tube end conditions used in the structural analysis of full tubes.

	Hot end displacement			Cold end displacement		
Tube (row)	Vertical (mm)	Radial (mm)	Rotation (radian)	Vertical (mm)	Radial (mm)	Rotation (radian)
Innermost (1)	−0.025	0.215	−0.001	0.025	0.215	0.001
Middle (25)	−0.254	2.658	−0.001	0.152	2.658	0.001
Outermost (49)	−0.515	5.100	−0.001	−0.356	5.100	0.001

3 THERMAL-STRUCTURAL ANALYSIS OF FULL U-TUBE MODELS

The above displacement response (of tubesheet) represents the net reaction of thermal-structural loads acting on the steam generator assembly as a unit. The tubes themselves are also subject to the differential thermal expansion along their lengths resulting from the expected temperature drop from hot leg to cold leg. These global actions induce local axial, bending, and shear loads at the *tube-to-tubesheet junction*. These loads, which are also affected by the prevailing constraints at various support plate intersections along a tube, are supported by the induced internal stresses within the tube section. The primary objective of this Section is to establish the magnitude of these stresses and to discuss the causative factors.

3.1 U-tube models and approach

The net deformation imposed by the tubesheet on a specific tube-end varies with the location of the tube; in addition, the length and U-bend radius of a tube are also dependent on the location. Therefore, three typical tubes, with somewhat arbitrary choice of locations, were selected for purposes of this analysis: the innermost tube (1st row), the middle tube (25th row), and the outermost tube (49th row) with U-bend radii of 5.715 cm, 70.485 cm, and 135.255 cm, respectively; all three were taken to be in the plane of half-symmetry (transverse to the divider plate). For the pre-heater type Model–D steam generator design of interest there are 8 full support plates covering both legs of the U-tubes and 6 partial supports covering only the cold leg portion.

Each of the selected tubes was analyzed individually. In order to account for the differential thermal expansion along the length of a tube, first the necessary temperature distributions were determined by considering the heat transfer across the tube-wall. Here the average through-wall temperatures are of importance. Due to the space limitation details of this heat transfer analysis are not included in this presentation. Very briefly, however, since most of the heat transfer in a tube is due to the (forced) convection in radial direction, a relatively simple one dimensional analysis was performed. The geometric and thermal-hydraulics parameters (design data) were representative of normal operating conditions for a typical Model–D type steam generator. To be conservative, the tube (heat transfer) surfaces were assumed *clean* (with no fouling).

The resulting average wall-temperatures and the previously determined tube-end displacements were used as inputs to the *structural* finite elements model of each tube to solve for the loads and displacements of interest. Finally, the loads are related to the corresponding tube stresses.

For the structural (load–displacement) analysis each tube was modeled as a series of beam elements (element type STIF3 of the LIBRA Code). The tube material is Ni-Cr-Fe Alloy 600 and the support plate material is plain carbon steel [SA-285 Gr.A].

The deformation of full tubes is restrained by the support plates with clearance holes through which the tubes pass; these holes are initially in approximate alignment with the corresponding holes in the tubesheet (here, the initial offset was assumed to be zero). The actual constraining conditions imposed by these plates on the tubes are unknown and are likely to be complex. Here, the supports are modeled with the following consideration: at each support the tube is assumed to be free to move axially and its (transverse) displacement in the plane of a support plate is restricted to be the same as that of the corresponding support hole. *i.e., the only load imposed by the supports is expected to be in the transverse direction.* The support plates themselves are assumed to move with very little thermal restraint so that they remain horizontal and expand radially depending on the average temperature at the corresponding location.

3.2 Results and discussion

The heat transfer analysis yielded mid-wall temperatures which show a nearly linear drop along the tube length; the total drop is about 10°K (18°F) for the shortest tube to about 12.5°K (22.5°F) for the longest tube (compared to the total drop of about 35°K [63°F] in the primary water).

The transverse (or radial) displacements of the center-lines of all three tubes are plotted in Fig. 3; here, the positive sign indicates displacement (measured from zero at the reference temperature of 294°K [70°F]) towards the shell side of the cold leg. It should be noted that the (magnified) plot of displacement is *not* the shape of the tube but a *change* in its original U-shape. Clearly, a relatively large *change of shape* is predicted, under the stated assumptions of this analysis, near the tubesheet and the first baffle plate, especially for the outer tubes, and also near the top two support plates and the U-bend region, especially for the inner tubes.

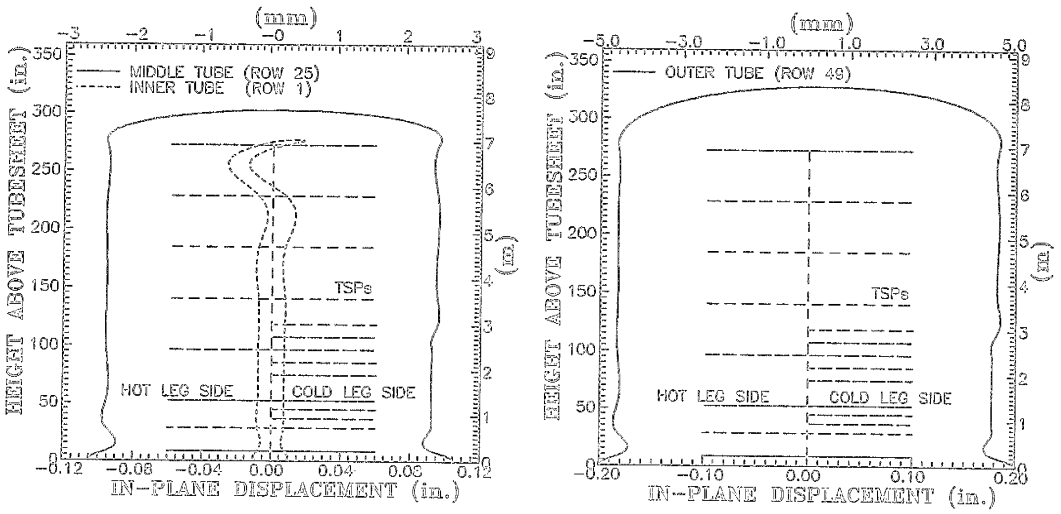

Fig. 3. Transverse displacements for three U-tubes. (Horizontal lines show the support plate locations).

Axial displacements (from the finite element analysis) for the three tubes compare well with simple hand calculations for thermal expansion using the temperature results of the tube heat transfer analysis. These displacements are nearly proportional to the height above the tubesheet.

The resultant reaction loads of interest are at the *tube-to-tubesheet* junctions on the hot and cold leg ends of tubes. These loads consist of an axial component, a shear component, and a bending moment, all acting on the transverse cross-section of a tube. The calculated loads from the finite element analysis of the three tubes are summarized in Table 2.

Table 2. Calculated reaction loads on the tube ends.

	Hot end loads			Cold end loads		
Tube (row)	Axial (N)	Shear (N)	Moment (N·m)	Axial (N)	Shear (N)	Moment (N·m)
Innermost (1)	71.30	47.46	8.51	71.30	48.57	8.64
Middle (25)	0.18	110.13	17.88	0.18	117.29	18.97
Outermost (49)	0.09	172.76	27.26	0.09	183.26	29.31

In this table the axial load on all hot legs is compressive and is tensile on cold legs; the shear loads on all ends are directed so as to separate the tube legs; also, the (in-plane, sectional) bending moment on all cross-sections is oriented so as to induce tension in the outer fibers (facing the shell side). Again, it is important to note that the three tubes selected for analysis are all located on the plane of half-symmetry of the steam generator.

The resulting stresses from these global thermal-structural reaction loads are considered in the following (for 19.05 mm [3/4 in.] tube OD with 1.0922 mm [0.043 in.] wall thickness):

(a) The axial load of 71 N (on the shortest radius U-tube) results in the nominal axial stress of 1.157 MPa in the straight section away from the tube-to-tubesheet junction. Near the junction, due to the sudden change in thickness, the classical discontinuity analysis suggests that the corresponding maximum axial stress is 3.592 MPa and the hoop stress is 1.545 MPa on the tube OD. This estimated maximum contribution is quite small. It is important to note, however, that the key assumption for this result to be valid in service is the *complete axial freedom* for the tubes to move in the support plate holes; any condition of locking at these holes (e.g. due to the corrosion products build-up) will result in increased axial stress. No attempt was made in this work to estimate such a locking stress.

(b) The distribution of tube stresses (and any stress concentration effect) at the joint, as induced by the transverse shear and the bending moment, is unknown. The *nominal* stress magnitudes, based on the simple elasticity theory of beam bending, are summarized in Table 3.

Table 3. Nominal stresses on the tube ends due to shear load and bending.

	Hot end peak stresses		Cold end peak stresses	
	Shear load	Bending	Shear load	Bending
Tube (row)	Shear (MPa)	Axial (MPa)	Shear (MPa)	Axial (MPa)
Innermost (1)	1.54	32.51	1.58	33.03
Middle (25)	3.58	68.30	3.81	72.48
Outermost (49)	5.61	104.13	6.04	111.98

Note that the maximum shear stress (in the transverse section of the tube due to the transverse shear load) is tangential to the tube perimeter and is located at 90 degree azimuth from where the bending axial stress is maximum; this contribution due to the shear load is relatively very small.

(c) The stresses due to section bending are dominant and are found to be higher for the outermost tubes. Although only *axial* component of the (nominal) stress is shown in Table 3, the *discontinuity effect* at the tubesheet junction is expected to produce some hoop stress. The corresponding (local) stress distribution and the expected stress concentration effect are unknown (for the tube). Also, it is important to note that the bending moment is dependent on hole clearances and the conditions of contacts at various support locations the actual details of which are not known with good accuracy or certainty. The above estimates of (nominal) bending stresses are likely to be conservative because of the assumption that transverse loads are applied by *all* the support plates. However, it should also be noted that the original hole clearances *are reduced* in service by the initial offsets (between the tubesheet holes and the support plate holes), the initial tube bowing, and the build-up of corrosion products. (In principle, assuming that realistic support conditions are known with enough accuracy, the static analysis for full U-tube model should be one of non-linear and iterative nature which was considered to be beyond the scope of this work).

Thus, tube stresses at the tubesheet junction were analyzed for the *global* thermal-structural reaction effects including tubesheet bending and displacements, in-plane displacements of support plates, and the differential thermal expansion of hot and cold legs of a tube. The stresses due to net (sectional) bending moment were found to dominate the global reaction at the tubesheet junction (provided the axial freedom of tubes is maintained) and the resultant peak stresses are of comparable magnitude to those (*local, axisymmetric*) stresses (Garud, 1991) due to the pressure and temperature differentials *across the tube-wall*. The large number and varied locations of tubes in any one steam generator suggest a large variation in the global reaction stresses is to be expected. Relatively high flexibility of the tube bundle and that of the shell structure were confirmed. Also, a relatively large change in the tube shape was found near the tubesheet and the first support plate for outer tubes and near the U-bend for inner tubes.

ACKNOWLEDGMENT

This work was sponsored by the Electric Power Research Institute (EPRI) of Palo Alto, California. The authors are grateful for the support provided by Dr. A. R. McIlree of EPRI. The 3D geometric model generation was greatly expedited by the special assistance provided by Dr. S. Kung of Phoebus Systems, Los Altos, California; the drawing for Fig. 1(b) is also courtesy of Dr. Kung.

REFERENCES

ASME (1980). Boiler and Pressure Vessel Code, American Society of Mechanical Engineers, New York.

Gardner, K. A. (1960). Heat-Exchanger Tube-Sheet Design—3. U-Tube and Bayonet-Tube Sheets. *Journal of Applied Mechanics*, ASME Transactions, March, pp. 25–33.

Garud, Y. S. (1991). Service Stresses Within the Expansion Transition of Tubes in a PWR U-tube Heat-exchanger Design Including Local Discontinuity and Geometry Effects. *Paper No. F15/3, 11th International Conference on SMiRT*, Tokyo, Japan, August.

S. Levy Incorporated. (1989). LIBRA Finite Element Code for PC.